

Survey of $\gamma p \rightarrow pK^+K^-\gamma\gamma$ events in GlueX

Sebastian Cole

Arizona State University

4/16/2021



U.S. DEPARTMENT OF
ENERGY



Jefferson Lab
Thomas Jefferson National Accelerator Facility

Table of contents

- 1 Motivation for the analysis of $\gamma p \rightarrow pK^+K^-\gamma\gamma$ events
 - 1.1 Previous experimental results
 - 1.2 Interpretation of previous 0^{-+} pseudoscalar results
- 2 Thomas Jefferson national accelerator facility
 - 2.1 The accelerator
- 3 The GlueX experiment
 - 3.1 The GlueX beamline
 - 3.2 The GlueX spectrometer
- 4 Analysis
 - 4.1 Event reconstruction
 - 4.2 Particle survey
- 5 Partial wave analysis
- 6 Motivation revisited

Table of Contents

- 1 Motivation for the analysis of $\gamma p \rightarrow pK^+K^-\gamma\gamma$ events
 - 1.1 Previous experimental results
 - 1.2 Interpretation of previous 0^{-+} pseudoscalar results
- 2 Thomas Jefferson national accelerator facility
 - 2.1 The accelerator
- 3 The GlueX experiment
 - 3.1 The GlueX beamline
 - 3.2 The GlueX spectrometer
- 4 Analysis
 - 4.1 Event reconstruction
 - 4.2 Particle survey
- 5 Partial wave analysis
- 6 Motivation revisited

The E/ι puzzle

Pseudoscalar in $\bar{p}p$ annihilation at rest

In 1963, E/ι peak at 1425 MeV seen in $K\bar{K}\pi$ mass spectrum [1].

E and ι separate particles

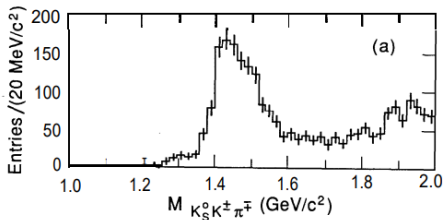
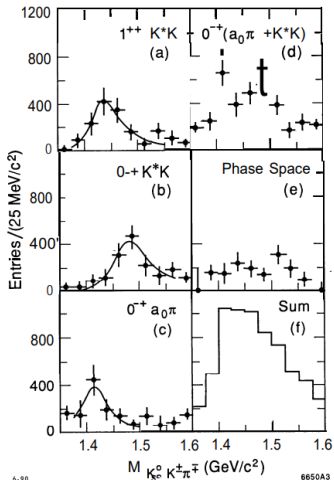
Different quantum numbers for different production mechanisms from spin-parity analysis, specifically the E meson 0^{-+} and the ι meson 1^{++} [2].

The 1998 PDG

The 1998 PDG reports an axial vector $f_1(1420)$ and pseudoscalar $\eta(1440)$ as the ι and E , respectively [3].

- [1] R. Armnteros *et al.*, Proc. of the Siena Int. Conf. on Elementary Particles I (1963) 287.
- [2] A. Bertin *et al.* (OBELIX), Phys. Lett. **B361**, 187 (1995).
- [3] R.M. Barnett *et al.*, Review of particle properties, Europ. Phys. Journal C3 (1998).

J/ψ decays at MARKIII

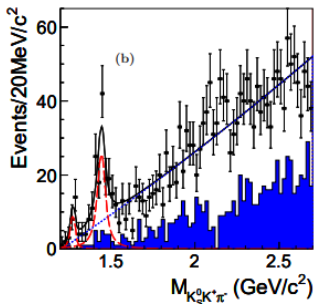
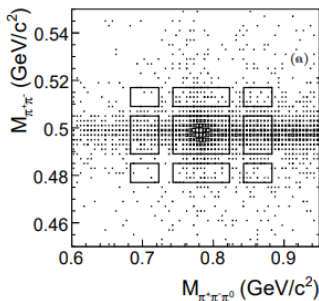


Two pseudoscalars in $K\bar{K}\pi$

Reported pseudoscalars at 1416 MeV and 1490 MeV decaying $a_0(980)\pi$ and $K^*(892)\bar{K}$ in J/ψ decays [1]. Confirmed by DM2 experiment.

[1] Z. Bai *et al.* (MARKIII), Phys. Rev. Lett. **65**, 2507 (1990).

J/ψ decays at BESII and BESIII



BESII mesons in $J/\psi \rightarrow \omega K \bar{K} \pi$ and $\phi K \bar{K} \pi$ decays

No evidence of meson states due to low statistics [1].

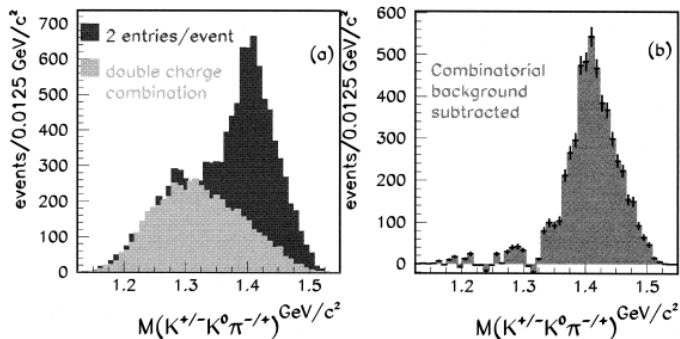
BESIII mesons in $\psi(3686) \rightarrow \omega K \bar{K} \pi$ decays

Evidence of mesons that could be $\eta(1405)$, $\eta(1475)$, and $f_1(1420)$ [2].

[1] M. Abilikin *et al.* (BES), Phys. Rev. **D77**, 032005 (2008), [arXiv:0712.1411].

[2] M. Abilikin *et al.* (BESIII), Phys. Rev. **D87**, 092006 (2013), [arXiv:1303.6360].

$p\bar{p}$ collisions in Obelix

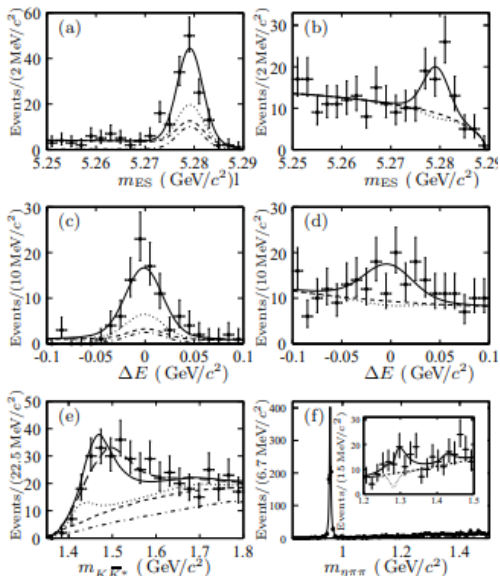


OBELIX evidence of two pseudoscalar states in 1.4 – 1.5 GeV region

In $p\bar{p}$ annihilation at rest, OBELIX shows evidence of two pseudoscalar mesons decaying $K\bar{K}\pi$ in the mass region of interest [1].

[1] C. Cicalo *et al.* (OBELIX), Phys. Lett. **B462**, 453 (1999)

B meson decays in BaBar

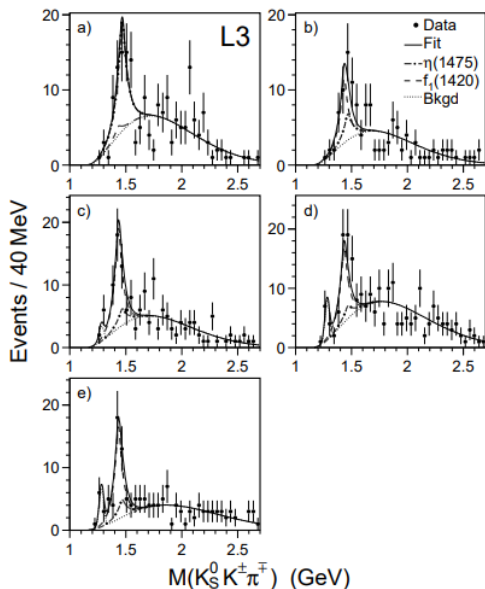


B-meson decay to $K\bar{K}^*K^+$

BaBar reports evidence of $\eta(1475)$ and $\eta(1295)$ in B^+ meson decay. Upper limits for $\eta(1405)$, $f_1(1285)$, $f_1(1420)$, and $\phi(1680)$ are also included.

- [1] B. Aubert *et al.* (BaBar), Phys. Rev. Lett. **101**, 091801 (2008), [arXiv:0804.0411].

$\gamma\gamma$ collisions in L3

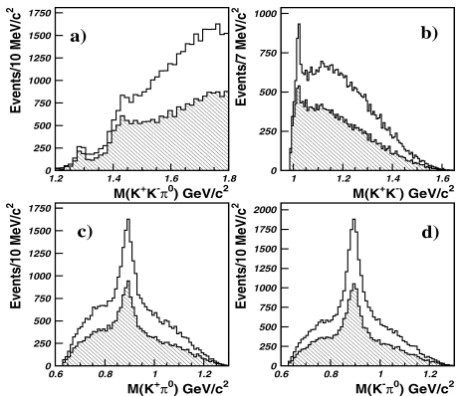


Evidence of $\eta(1475)$ in $\gamma\gamma$ collisions

The L3 collaboration shows evidence of $\eta(1475)$ in $\gamma\gamma$ collisions, but not the $\eta(1405)$. This supports the argument that $\eta(1405)$ consists only of gluonic content [1].

[1] P. Achard *et al.* (L3), JHEP **03**, 018 (2007)

E852 at Brookhaven invariant mass distributions



18 GeV π^- beam experiment

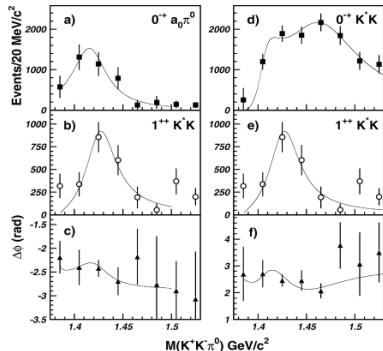
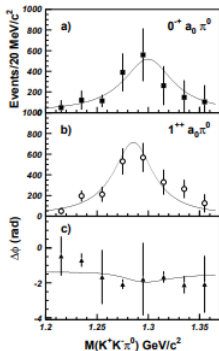
Kinematically fit results for $\pi^- p \rightarrow K \bar{K} \pi^0 n$ events from the E852 experiment at Brookhaven National Laboratory (BNL) performed in 1997 [1].

[1] G.S. Adams *et al.*, Phys. Lett. **B516**, 264, 2001.

$K^+ K^- \pi^0$ invariant mass distribution

Visible peaks from multiple overlapping meson states (top left). Partial wave analysis (PWA) required to identify the particles by their J^{PC} quantum numbers [1].

E852 at Brookhaven PWA results



PWA of $K^+K^-\pi^0$

Evidence of $\eta(1295)$ and $f_1(1285)$ decay $a_0(980)\pi^0$ left. Evidence of $\eta(1416)$ decay $a_0(980)\pi^0$ and $K^*\bar{K}$, and $\eta(1485)$ and $f_1(1420)$ decay $K^*\bar{K}$ right [1].

[1] G.S. Adams *et al.*, Phys. Lett. **B516**, 264, 2001.

Interpretation of previous results

The $\eta(1295)$ and $\eta(1475)$ pseudoscalars

The existence of the $\eta(1295)$ seen in $\pi^- p$, J/ψ decays, and B meson decays is debated. Assuming the $\eta(1295)$ exists, then it may be the first radial excitation of η and the $\eta(1475)$ is the first radial excitation of η' . The $\eta(1475)$ isoscalar would be the $s\bar{s}$ contribution to the 0^{-+} nonet [1].

The $\eta(1405)$ pseudoscalar

If two pseudoscalar mesons exist in the 1400 MeV region, the $\eta(1405)$ might be something other than a meson, specifically 0^{-+} glueball. This is supported by the fact that it is not seen in $\gamma\gamma$ collisions in L3. This is not supported by lattice gauge theory, but is by the flux tube model [2][3].

[1] T. Gutsche *et al.*, Phys. Rev. **D79**, 014036 (2009), [arXiv:0811.0668].

[2] C. J. Morningstar *et al.*, Phys. Rev. **D60**, 034509 (1999), [hep-lat/9901004].

[3] L. Faddeev *et al.*, Phys. Rev. **D70**, 114033 (2004), [hep-ph/0308240].

Motivation for the analysis of $\gamma p \rightarrow pK^+K^-\gamma\gamma$ events

- 1 Do two pseudoscalar mesons exist in the 1400 MeV region seen in production mechanisms: $\pi^- p$, radiative $J/\psi(1S)$ decay, and $\bar{p}p$ annihilation at rest?

Pseudoscalar decays

$$\eta(1405) \rightarrow a_0(980)\pi^0$$

$$\eta(1405) \rightarrow K\bar{K}\pi$$

$$\eta(1475) \rightarrow K^*(892)\bar{K}$$

- 2 Does GlueX observe the η'_1 hybrid meson candidate at ~ 2.3 GeV, which adds a member to the 1^{-+} nonet?

Hybrid meson candidate decays

$$\eta'_1 \rightarrow K^*(892)\bar{K}$$

$$\eta'_1 \rightarrow K_1^*(1410)\bar{K}$$

Table of Contents

- 1 Motivation for the analysis of $\gamma p \rightarrow pK^+K^-\gamma\gamma$ events
 - 1.1 Previous experimental results
 - 1.2 Interpretation of previous 0^{-+} pseudoscalar results
- 2 Thomas Jefferson national accelerator facility
 - 2.1 The accelerator
- 3 The GlueX experiment
 - 3.1 The GlueX beamline
 - 3.2 The GlueX spectrometer
- 4 Analysis
 - 4.1 Event reconstruction
 - 4.2 Particle survey
- 5 Partial wave analysis
- 6 Motivation revisited

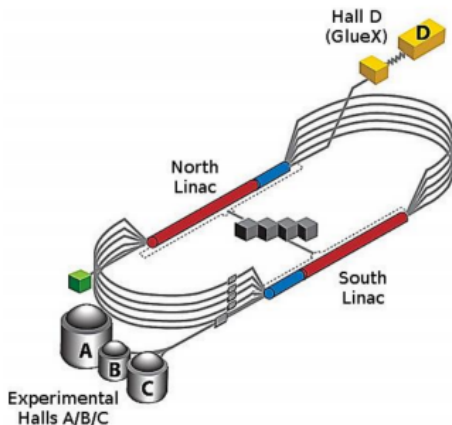
Thomas Jefferson national accelerator facility



Jefferson lab

Located in Newport News, Virginia, Jefferson Lab is home to an electron accelerator that support four experimental halls.

The continuous electron beam accelerator facility



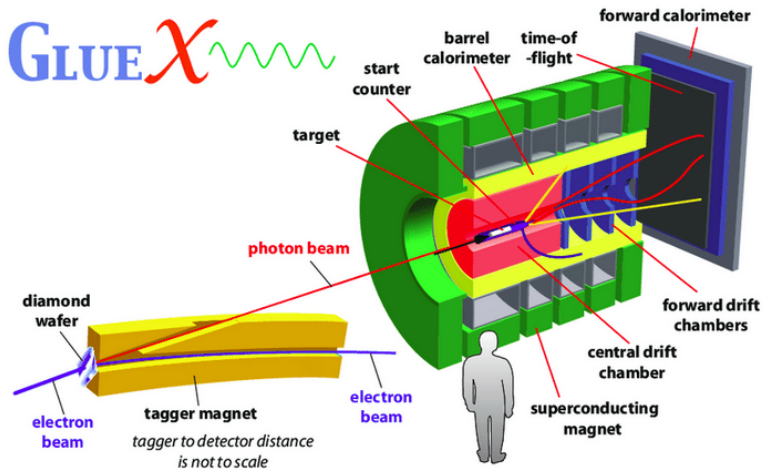
Continuous electron beam accelerator facility (CEBAF)

CEBAF consists of two linacs making an ~ 1.4 km racetrack shaped, electron accelerator capable of producing an ~ 12 GeV electron beam.

Table of Contents

- 1 Motivation for the analysis of $\gamma p \rightarrow pK^+K^-\gamma\gamma$ events
 - 1.1 Previous experimental results
 - 1.2 Interpretation of previous 0^{-+} pseudoscalar results
- 2 Thomas Jefferson national accelerator facility
 - 2.1 The accelerator
- 3 The GlueX experiment
 - 3.1 The GlueX beamline
 - 3.2 The GlueX spectrometer
- 4 Analysis
 - 4.1 Event reconstruction
 - 4.2 Particle survey
- 5 Partial wave analysis
- 6 Motivation revisited

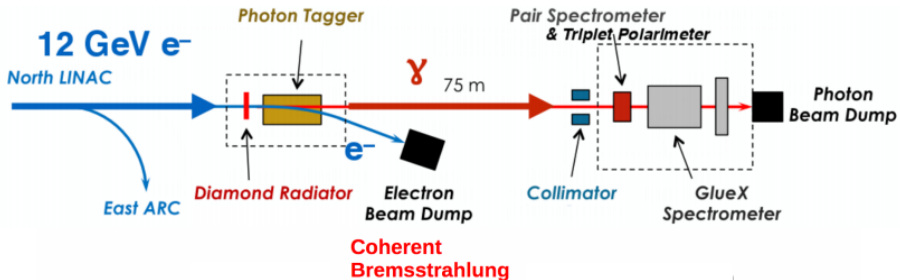
The GlueX experiment



Goal

The GlueX experiment aims to map the light meson spectrum.

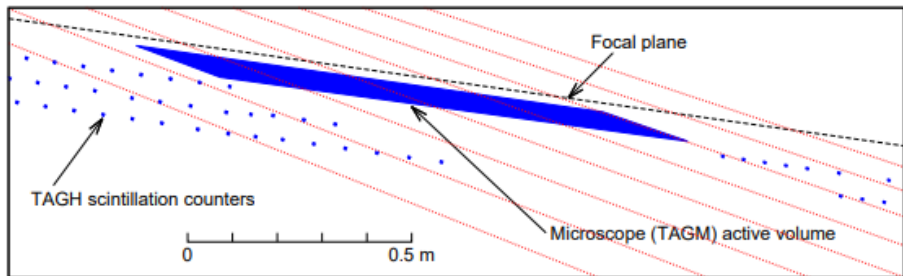
The GlueX Bremsstrahlung photon beamline



beamline overview

The GlueX beamline consists of a thin diamond radiator held by a goniometer from which a polarized photon beam is created through the Bremsstrahlung process. Scintillating detectors are used to reconstruct the photon beam energies and a silicon strip detector is used to determine photon beam polarization.

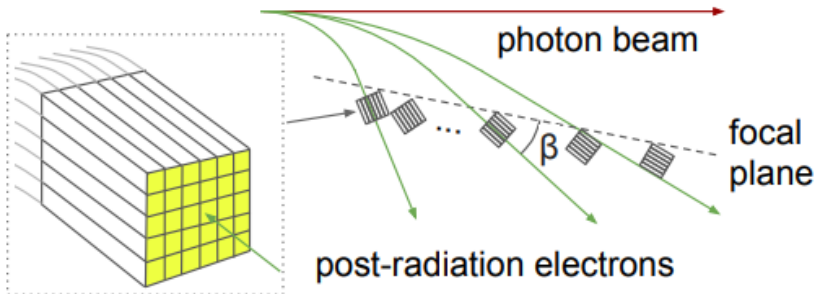
Tagger hodoscope (TAGH)



Hodoscope

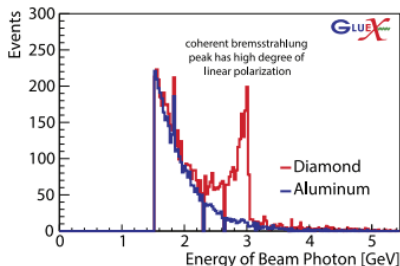
Scintillating detector that detects accelerator electrons to reconstruct photons with energies outside the coherent peak from 3.05 – 8.10 GeV and 9.10 – 11.78 GeV.

Tagger microscope (TAGM)

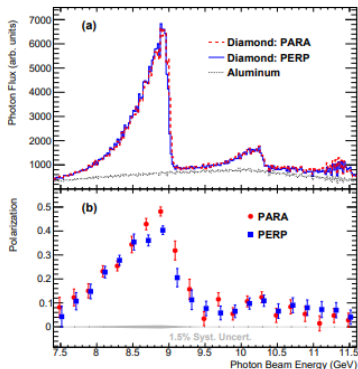


Microscope

Scintillating detector that detects accelerator electrons to reconstruct photons with energies within the coherent peak, where polarized photons are expected.



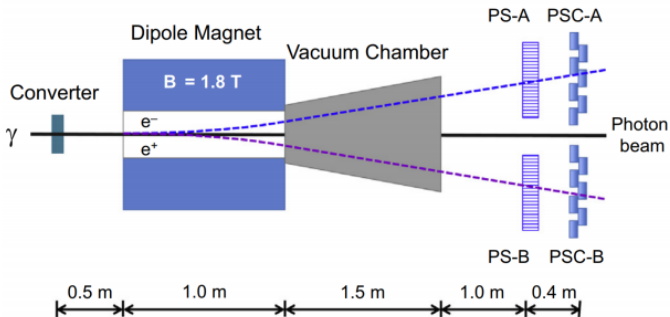
Triplet polarimeter (TPOL)



Photon beam polarization

TPOL detects recoil electrons ejected from beryllium foil with large opening angles due to interaction with the incident photon beam. The azimuthal distribution of these electrons is used to determine the incident photon beam polarization.

Pair spectrometer (PS)



Beamline trigger

The PS is a scintillating detector used as a triggering system and calibration tool for the beamline.

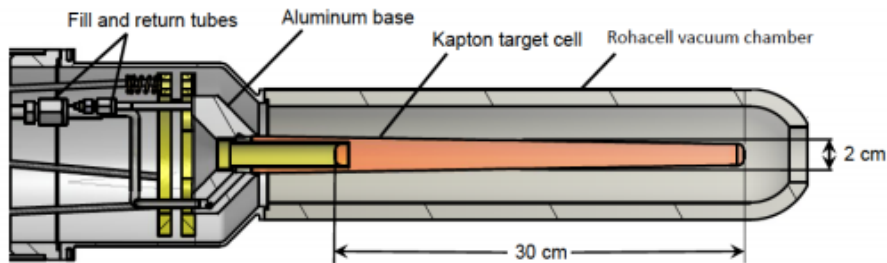
The GlueX spectrometer



GlueX spectrometer overview

The GlueX spectrometer consists of six sub-detectors. A cryogenic hydrogen target is inserted into a tracking volume such that it is surrounded by the central drift chamber, the barrel calorimeter, and a superconducting solenoid. The forward drift chamber caps the downstream end of the tracking volume. The forward calorimeter and time of flight planar detectors cover the downstream end of the hall.

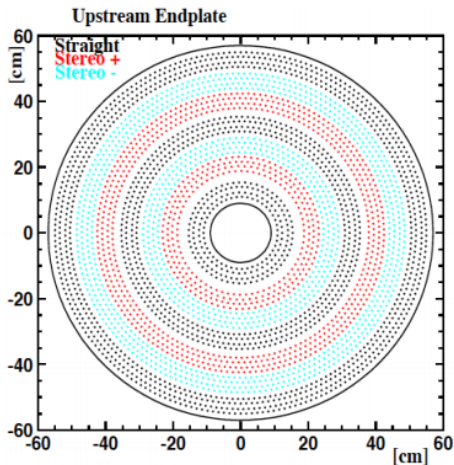
Target



Cryogenic hydrogen

GlueX is a photoproduction experiment that uses a cone-like, liquid hydrogen target, since this consists mainly of protons.

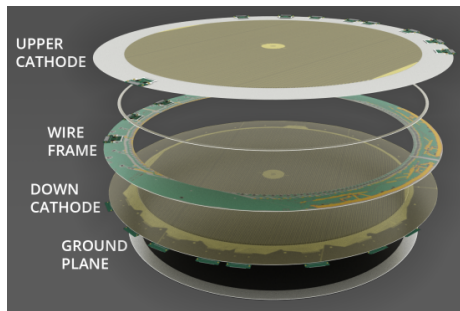
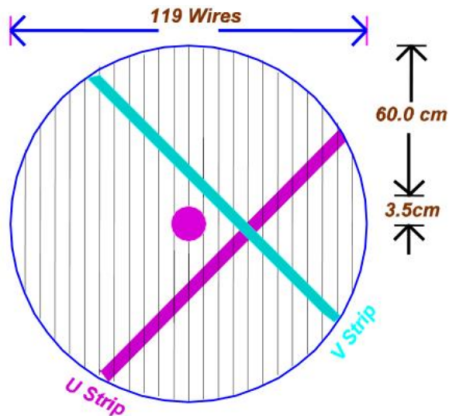
Central drift chamber (CDC)



CDC

The CDC consists of 3,522, 1.5 m long, mylar Lamina straw tubes arranged cylindrically over 28 layers, 12 axial and 16 stereo.

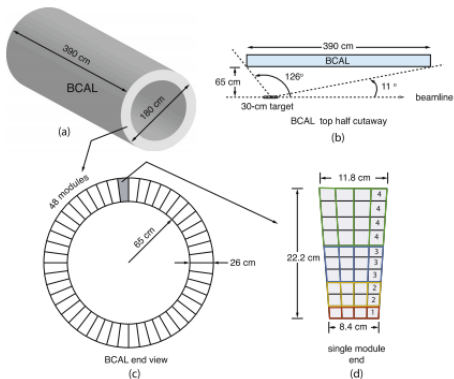
Forward drift chamber (FDC)



FDC

The FDC consists of four circular planes made of six flat drift chambers offset by an azimuthal angle of 60° .

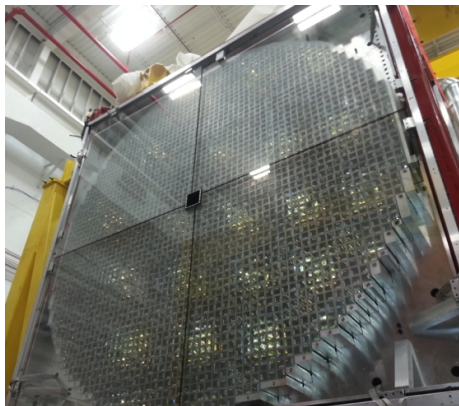
Barrel calorimeter (BCAL)



BCAL

BCAL is a cylindrical calorimeter that surrounds the tracking volume with 48 trapezoidal modules. Charged and neutral particles are reconstructed from their electromagnetic showers.

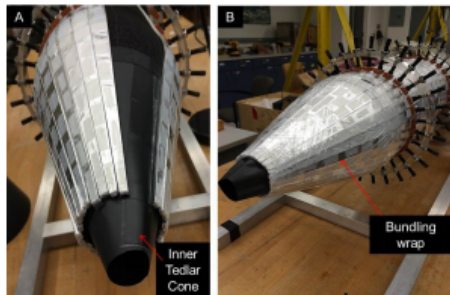
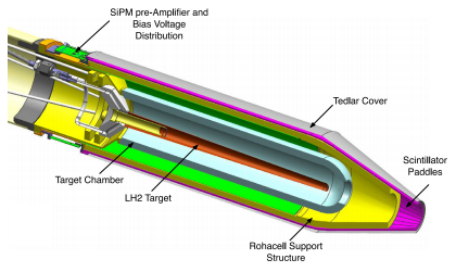
Forward calorimeter (FCAL)



FCAL

FCAL consists of 2800 decommissioned, lead glass blocks arranged in a circle to make a plane that detects electromagnetic showers of charged and neutral particles.

Start counter (ST)



ST

The ST surrounds the target with scintillating paddles. It is used to obtain start times of events in coincidence with beam photons.

The time of flight (TOF)



TOF

TOF consists of 46 scintillating paddles arranged in a plane such that it has a vertical and horizontal layer.

Table of Contents

- 1 Motivation for the analysis of $\gamma p \rightarrow pK^+K^-\gamma\gamma$ events
 - 1.1 Previous experimental results
 - 1.2 Interpretation of previous 0^{-+} pseudoscalar results
- 2 Thomas Jefferson national accelerator facility
 - 2.1 The accelerator
- 3 The GlueX experiment
 - 3.1 The GlueX beamline
 - 3.2 The GlueX spectrometer
- 4 Analysis
 - 4.1 Event reconstruction
 - 4.2 Particle survey
- 5 Partial wave analysis
- 6 Motivation revisited

Goal I

Add to the debate over the existence of two pseudoscalar mesons in the 1400 MeV region seen in three production mechanism thus far.

Goal II

Search for evidence of the η_1' hybrid meson candidate decaying $K^*(892)\bar{K}$ and/or $K_1^*(1401)\bar{K}$.

Reconstruction

Charged particles

Charged particles are reconstructed using a helical fit of their points of detection in the CDC and other detectors. This fit is dependent on the assumed identification of a particle. If the fit converges, the identification hypothesis and its respective kinematic information is kept.

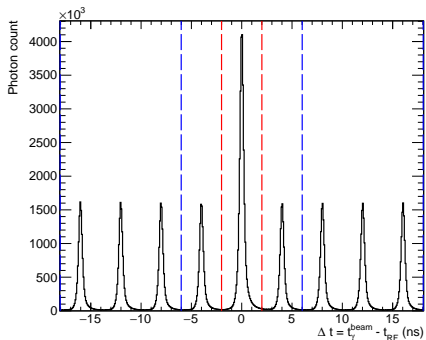
Neutral particles

Neutral particles are reconstructed using their electromagnetic showers in BCAL and FCAL.

Events

Events are produced based on combinations of the charged tracks and neutrals, coupled with the beam photons in time with the event. This is a combinatorial problem since the selection of charged and neutral particles comes from a set larger than what is required for a reaction.

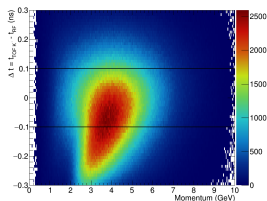
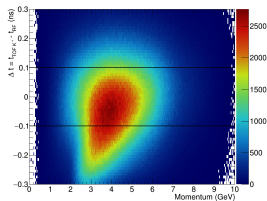
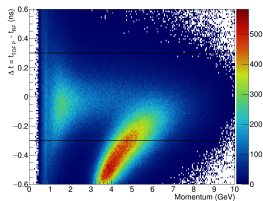
Beam photons



Beam photon selection

Beam photons in time with detected events fall between -2.004 and 2.004 ns, surrounded by side-band peaks from out of time beam photons. Combinations with signal peak photons are given a weight of $1/N_{\gamma,i}$ and combinations with side-band photons are given a weight of $-f/(N_a N_{\gamma,i})$, where $N_{\gamma,i}$ is the number of times a photon is used, N_a is the number of accidental side-bands used, and f is a correction factor.

Selection of tracks in time with beam photons

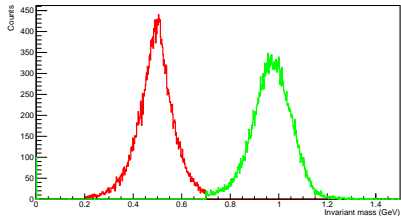
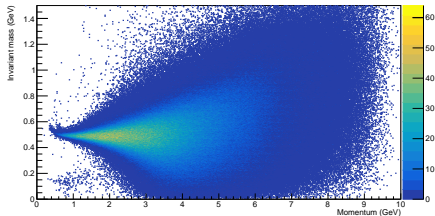


Δt for a charged tracks or neutrals

The time for an event at the vertex is determined by propagating back to the vertex within the target volume. From the tracking reconstruction, it is possible to determine the time an event occurs for each particle hypothesis. The distribution is centered over zero for the correct particle identification.

Detector	Δt_p (ns)	Δt_{K^\pm} (ns)	Δt_γ (ns)
BCAL	± 0.5	± 0.2	± 2.0
FCAL	± 1.0	± 0.5	± 2.0
TOF	± 0.3	± 0.15	NA
ST	None	None	NA
NULL	None	None	NA

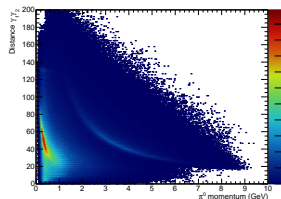
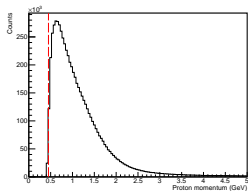
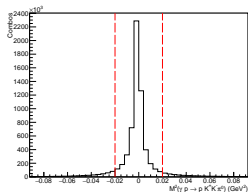
Problem with particle identification



Poor kaon PID for high momentum kaon

Reactions with kaon contributions in pre-DIRC GlueX data succumb to large pion contamination. The left plot shows the invariant mass versus momentum for charged tracks identified as K^+ by the tracking reconstruction after a confidence level cut on the kinematic fit. The right plot shows the invariant mass of the K^+ and p charged tracks after all the cuts and requiring that kaons have momentums less than 3 GeV.

Event selection



Removal conditions

Confidence level kin-fit $< 10^{-3}$

$$\theta_\gamma < 1.5^\circ$$

$$10.3^\circ > \theta_\gamma < 11.5^\circ$$

$$E_{BCAL}^{min} < 0.05 \text{ GeV}$$

Shower quality FCAL < 0.5

$$d_{\gamma_1, \gamma_2} < 12.5 \text{ cm}$$

$$MM^2 > 0.2 \text{ GeV}$$

$$p_p^{recoil} < 0.45 \text{ GeV}$$

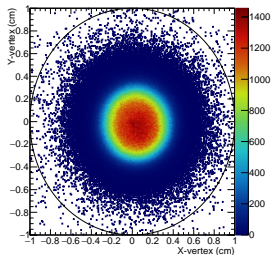
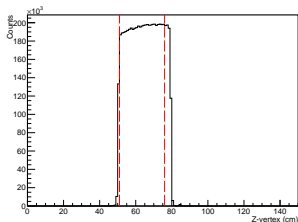
$$52 \text{ cm} < z_{vertex} > 78 \text{ cm}$$

$$r_{vertex} > 1 \text{ cm}$$

Selection of combinations

Combinations in an event are selected meeting the criteria to the left.

Kinematic fitting



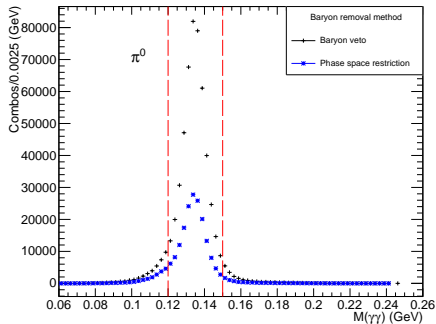
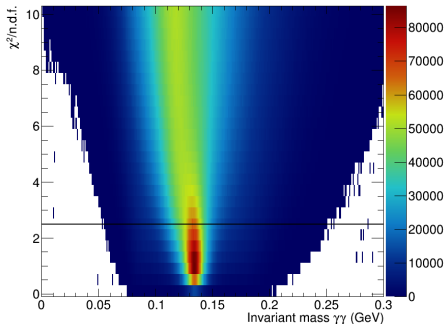
Kinematic fitter

A four-momentum and vertex kinematic fit is performed through a χ^2 minimization, determined by

$$\chi^2 = (\eta_0 - \eta_f)^T G_y (\eta_0 - \eta_f)$$

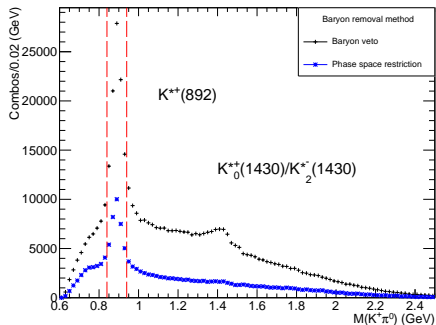
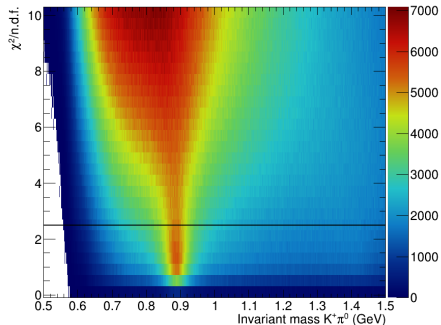
where η_0 is the vector of the quantity values before the fit, η_f is the vector of the quantity values after the fit, and G_y is the inverse of the covariance matrix for those quantities.

$$\pi^0 \rightarrow \gamma\gamma$$



π^0 selection

From Gaussian with third degree polynomial fit, π^0 mesons is selected using 2σ from center, 0.12 – 0.15 GeV as shown by dashed lines.



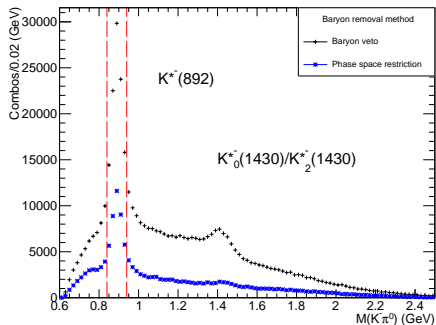
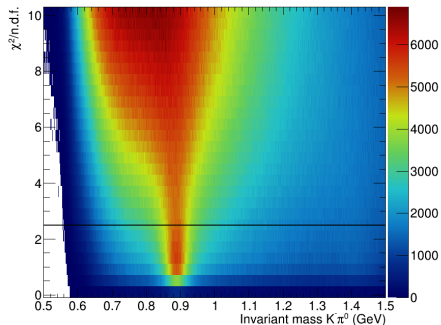
$K^{*+}(892)$ selection

From Gaussian with third degree polynomial fit, $K^{*+}(892)$ mesons is selected using 2σ from center, 0.84 – 0.94 GeV as shown by dashed lines.

Excited K^*

A peak for excited K^* mesons near ~ 1.4 GeV is visible. This may include $K_1^*(1410)$, predicted to be an η_1' hybrid meson candidate decay product.

$$K^{*-}(892) \rightarrow K^{-}\pi^0$$



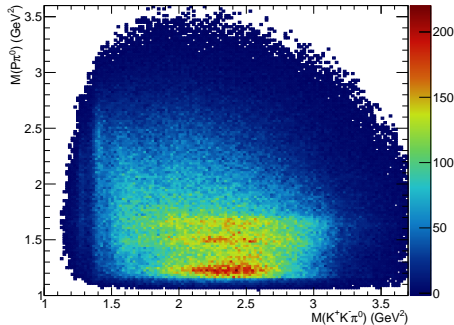
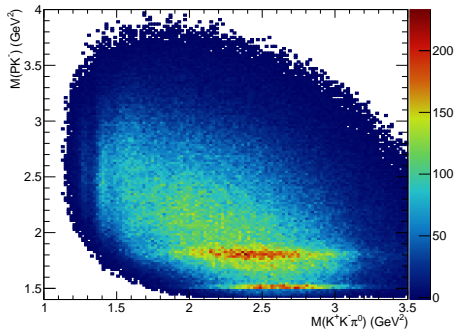
$K^{*-}(892)$ selection

From Gaussian with third degree polynomial fit, $K^{*-}(892)$ mesons are selected using 2σ from center, 0.84 – 0.94 GeV as shown by dashed lines.

Excited K^*

A peak for excited K^* mesons near ~ 1.4 GeV is visible. This may include $K_1^*(1410)$, predicted to be an η_1' hybrid meson candidate decay product.

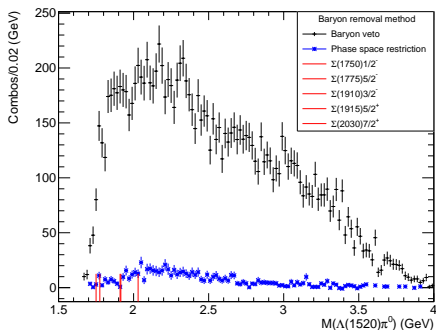
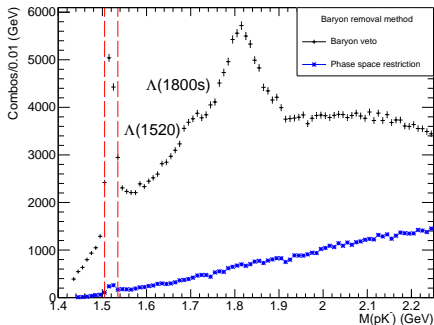
Baryon background contributions



Veto versus phase space restriction

Baryons make up a large background contribution to mesons decaying $K^+K^-\pi^0$ as seen in the plots above. This is reduced in two ways: through a mass veto or by a phase space restriction. The phase space restriction greatly reduces the baryon background and is a better option for further analysis.

$\Lambda(1520)\pi^0 \rightarrow pK^-\pi^0$

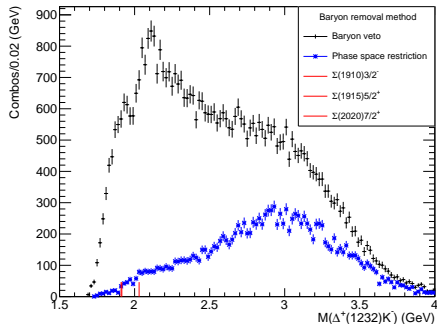
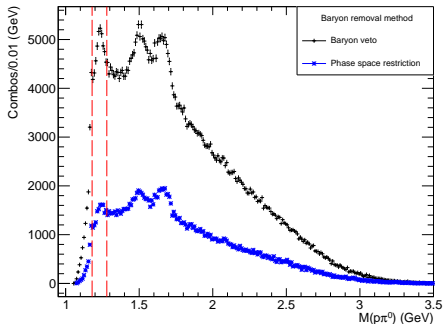


$\Lambda(1520) \rightarrow pK^-$ selection

From Gaussian with third degree polynomial fit, $\Lambda(1520)$ baryons are selected using 2σ , 1.505 – 1.535 GeV as shown by dashed lines.

Σ baryons

Possible evidence of $\Sigma(1750)$ and $\Sigma(1775)$, as well as peaks near ~ 2.15 GeV and ~ 2.3 GeV for possible baryons not reported by the PDG.



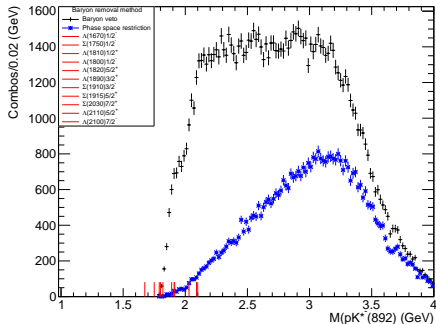
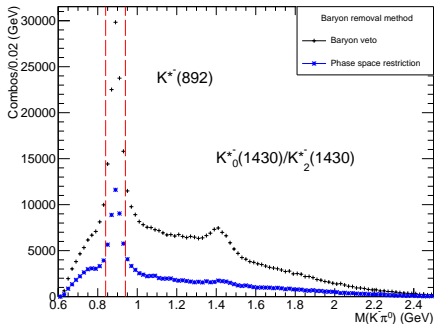
$\Delta^+(1232) \rightarrow p\pi^0$ selection

From Gaussian with third degree polynomial fit, $\Delta^+(1232)$ baryons are selected using 2σ , 1.180 – 1.280 GeV as shown by dashed lines.

Σ baryons

Possible evidence of $\Sigma(1910)$ and $\Sigma(1915)$, as well as peaks near ~ 2.65 GeV for possible baryon not reported by the PDG.

$$pK^{*-}(892) \rightarrow pK^{-}\pi^0$$



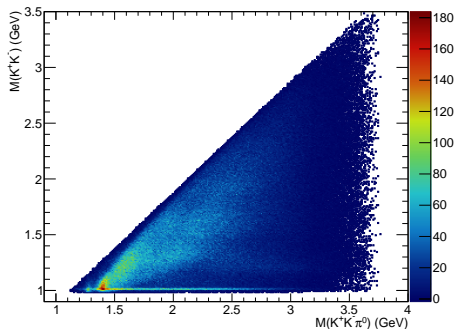
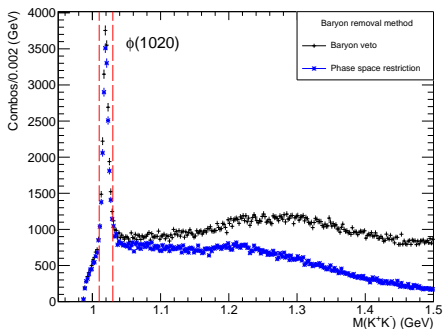
$K^{*-}(892) \rightarrow K^{-}\pi^0$ selection

From Gaussian with third degree polynomial fit, $K^{*-}(892)$ mesons are selected using 2σ from center, $0.84 - 0.94$ GeV as shown by dashed lines.

Σ and Λ baryons

Possible evidence of $\Lambda(1890)$, $\Sigma(1910)$, and $\Sigma(1915)$, as well as peaks near ~ 2.5 GeV, ~ 3.0 GeV, ~ 3.1 GeV, and ~ 3.2 GeV not in the PDG.

$\phi(1020)\pi^0 \rightarrow K^+K^-\pi^0$



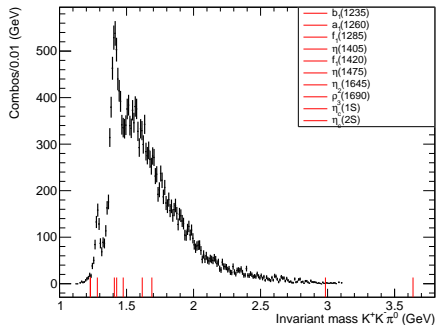
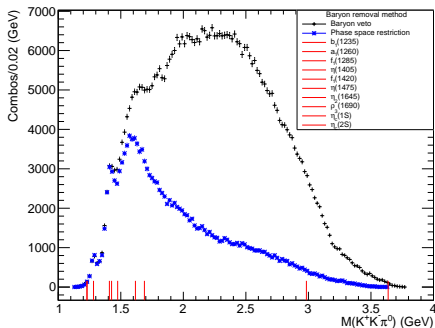
$\phi(1020) \rightarrow K^+K^-$ selection

From Gaussian with third degree polynomial fit, $\phi(1020)$ mesons are vetoed using 2σ from center, 1.01 – 1.03 GeV as shown by dashed lines.

$a_0(980)\pi^0$ decay

Evidence of possible $f_1(1285)$, $\eta(1295)$, and $\eta(1405)$ decaying $a_0(980)\pi^0$ from the enhancements in the bottom left corner of left plot.

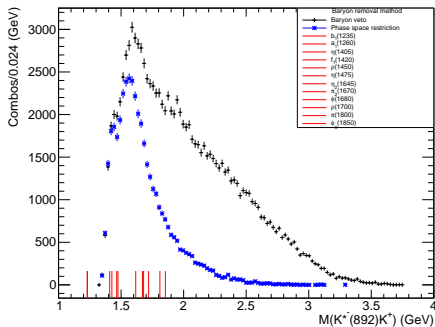
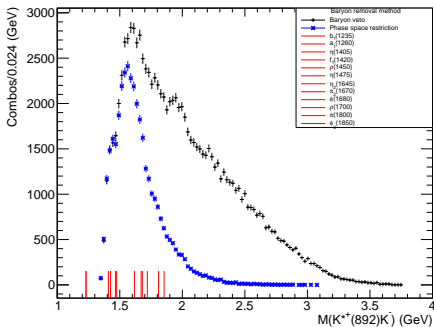
$$X \rightarrow K^+ K^- \pi^0$$



Possible meson states

The $f_1(1285)$ meson is believed to be major contributor to the left most peak because it has a width of ~ 22.7 MeV. The $\eta(1405)$ meson is believed to be the major contributor to the second peak because it has a width of ~ 84.59 MeV. Full PWA for the three-body decay required for confirmation. No conclusive evidence of η_c for what is the most likely decay to see this charmed meson in GlueX data.

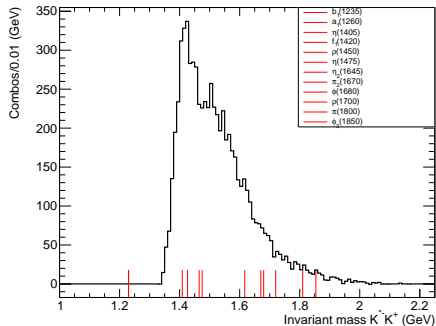
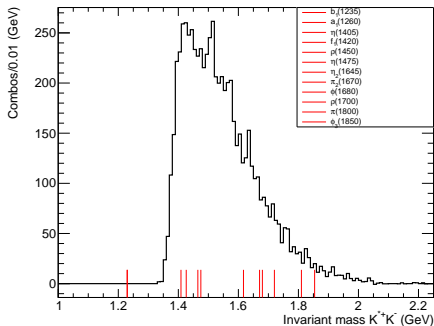
$$X \rightarrow K^{*\pm}(892)K^{\mp}$$



Possible meson states

Visible peak near ~ 1.4 GeV for both distributions. This is consistent with $\eta(1405)$, $f_1(1420)$, $\rho(1450)$, and $\eta(1475)$. Difficult to make any other conclusions for higher mass peaks without PWA.

$X \rightarrow K^{\pm*}(892)K^{\mp}$ for only TOF detected $p_{K^{\pm}} < 3.0$ GeV



Reduction of pion contamination

Pion contamination is greatly reduced by requiring kaons be detected by TOF and have momentum less than 3 GeV. Confirms possible meson states around 1400 MeV.

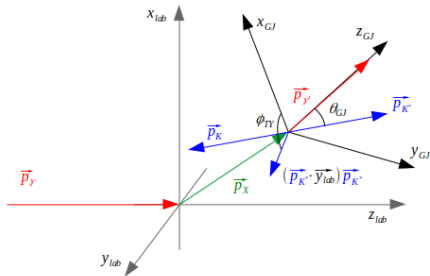
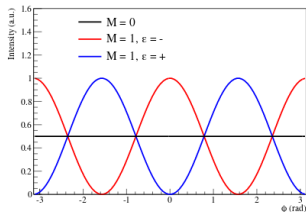
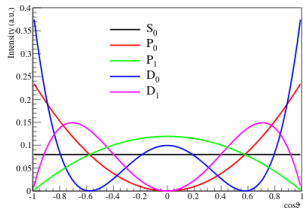
Table of Contents

- 1 Motivation for the analysis of $\gamma p \rightarrow pK^+K^-\gamma\gamma$ events
 - 1.1 Previous experimental results
 - 1.2 Interpretation of previous 0^{-+} pseudoscalar results
- 2 Thomas Jefferson national accelerator facility
 - 2.1 The accelerator
- 3 The GlueX experiment
 - 3.1 The GlueX beamline
 - 3.2 The GlueX spectrometer
- 4 Analysis
 - 4.1 Event reconstruction
 - 4.2 Particle survey
- 5 Partial wave analysis
- 6 Motivation revisited

Partial wave analysis

Fit angular distribution

Apply fits using spherical harmonics to mass dependent angular distributions in the GJ frame.



Gottfried-Jackson frame (GJ)

In rest frame of meson:
z-direction - photon beam direction
y-direction - $y = \vec{p}_\gamma^{beam} \times \vec{p}_{meson}$
x-direction - right handed system.

Intensity in reflectivity bases

The intensity for amplitude analysis is defined over a phase space τ . A are the wave contributions and ρ is the resonance spin density matrix, with V being the production amplitudes determined by fitting. (k is the rank of the spin density matrix element) Issue here is this is for X decaying to spinless mesons, which may work for $a_0(980)\pi^0$ decays, but not for $K^*(892)\bar{K}$ decays [1].

$$\begin{aligned} I(\tau) &= \frac{d\sigma}{dtdm} \\ &= \sum_k \sum_{\epsilon\epsilon'} \sum_{b,b'} \epsilon A_b \epsilon V_b^k \rho_{\epsilon,\epsilon'} \epsilon' V_{b'}^{k*} \epsilon' A_{b'}^*(\tau) \end{aligned}$$

[1] C. Salgado and D. Weygand, arXiv:1310.7498 (2013).

Phase space Monte Carlo

MC generation

Phase space MC is built using an amplitude generator. A flat phase space distribution with $t_{slope} = 3.0 \text{ GeV}^2$ for $\gamma p \rightarrow pK^+K^-\gamma\gamma$ is produced where $a_0(980) \rightarrow K^+K^-$, $\phi(1020) \rightarrow K^+K^-$, and $K^{*\pm}(892) \rightarrow K^\pm\pi^0$ resonances are included for the production of mesons that undergo a two body decay.

Particle modelling

The $\phi(1020)$ and $K^*(892)$ are modeled using Breit-Wigners with center and width obtained from PDG. The width of the ϕ may need to be updated to match the GlueX data. The $a_0(980)$ suffers from being near threshold, therefore a Flatte parametrization is used to model its line shape [1].

$$F_{K\bar{K}} = \frac{g_{K\bar{K}}}{m_{a_0}^2 - m^2 - i(\rho_{\eta\pi}(m)g_{\eta\pi}^2 + \rho_{K\bar{K}}(m)g_{K\bar{K}}^2)}, \quad \rho_i(m) = \frac{2q(m)}{m}$$

[1] C. Meyer, GlueX-Doc:4825 (2020).

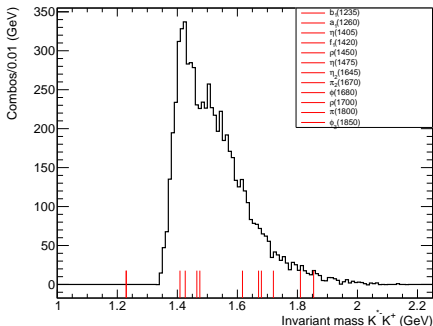
Table of Contents

- 1 Motivation for the analysis of $\gamma p \rightarrow pK^+K^-\gamma\gamma$ events
 - 1.1 Previous experimental results
 - 1.2 Interpretation of previous 0^{-+} pseudoscalar results
- 2 Thomas Jefferson national accelerator facility
 - 2.1 The accelerator
- 3 The GlueX experiment
 - 3.1 The GlueX beamline
 - 3.2 The GlueX spectrometer
- 4 Analysis
 - 4.1 Event reconstruction
 - 4.2 Particle survey
- 5 Partial wave analysis
- 6 Motivation revisited

Motivation revisited

An onerous debate

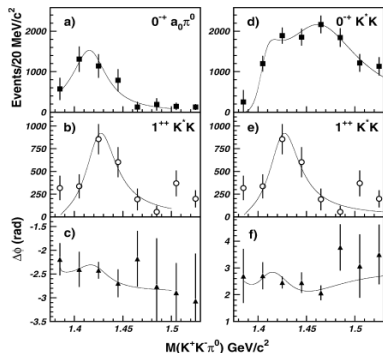
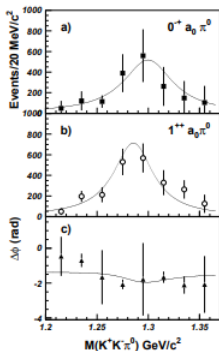
The GlueX experiment shows a peaking structure in the 1400 MeV mass region. This is consistent with results dating back to the 1960s. An onerous debate over what particles contribute to this distribution has continued for 60 years. Does the GlueX data show two pseudoscalars? Can GlueX help settle the debate over the quark and gluonic structure of $\eta(1295)$, $\eta(1405)$, and $\eta(1475)$?



η' hybrid meson candidate

Beyond the absolutely necessary work of contributing to the ongoing debate, can GlueX provide evidence of the η' hybrid meson candidate?

PWA goal



Future PWA

Near future work on PWA of the $a_1(980)\pi^0$ and $K^*(892)\bar{K}$ should be similar to that of the E852 results above. This work should assist in making conclusions about the quark-gluon content of the pseudoscalars in this decay mode [1].

[1] G.S. Adams *et al.*, Phys. Lett. **B516**, 264, 2001.

Possible expected states from 2018 PDG

Particle	$I^G(J^{PC})$	Decays	Mass (MeV)	Width (MeV)
$b_1(1235)$	$1^+(1^{+-})$	$K^+K^-\pi^0/K^{*\pm}K^{\mp\dagger}$	1229.5 ± 3.2	142 ± 9
$a_1(1260)$	$1^-(1^{++})$	$K^{*\pm}K^{\mp\dagger}$	1230 ± 40	$250 - 600$
$f_1(1285)$	$0^+(1^{++})$	$K^+K^-\pi^0$	1281.9 ± 0.5	22.7 ± 1.1
$\eta(1405)$	$0^+(0^{-+})$	$K^+K^-\pi^0\dagger/K^{*\pm}K^{\mp\dagger}$	1408.8 ± 1.8	51.0 ± 2.9
$f_1(1420)$	$0^+(1^{++})$	$K^+K^-\pi^0\dagger/K^{*\pm}K^{\mp\dagger}$	1426.4 ± 0.9	54.9 ± 2.6
$f_1(1450)$	$1^+(1^{--})$	$K^{*\pm}K^{\mp*}$	1476 ± 4	85 ± 9
$\eta_2(1645)$	$0^+(2^{-+})$	$K^+K^-\pi^0\dagger/K^{*\pm}K^{\mp\dagger}$	1617 ± 5	181 ± 11
$\pi_2(1670)$	$1^-(2^{-+})$	$K^{*\pm}K^{\mp\dagger}$	1672.2 ± 3.0	260 ± 9
$\phi(1680)$	$0^-(1^{--})$	$K^{*\pm}K^{\mp\dagger}$	1680 ± 20	150 ± 50
$\rho_3(1690)$	$1^+(3^{--})$	$K^+K^-\pi^0$	1688.8 ± 2.1	161 ± 10
$\rho(1700)$	$1^+(1^{--})$	$K^{*\pm}K^{\mp\dagger}$	1720 ± 20	250 ± 100
$\phi(1850)$	$0^-(3^{--})$	$K^{*\pm}K^{\mp\dagger}$	1854 ± 7	$87 \pm 28/23$

If no marker on the decay(s), has defined branching fraction.

* - possibly seen

† - seen

‡ - dominant

Work cited for detector section

- [1] Y. Qiang *et al.* (SOLID), Nucl. Instrum. Methods **B350**, 71 (2015).
- [2] S. Adhikari *et al.* (GlueX), Nucl. Instrum. Methods **A987**, 164807 (2021).